Available online at www.sciencedirect.com
SCIENCE DIRECT®
Journal of Power Sources 144 (2005) 1–10
JOURNAL OF POWER SOURCES
www.elsevier.com/locate/jpowsour

Synthesis, characterization and electrochemical studies of Ti-incorporated tungsten trioxides as platinum support for methanol oxidation

V. Raghuveer, B. Viswanathan*

Department of Chemistry, Indian Institute of Technology, Madras, Chennai 600036, India

Received 18 October 2004; accepted 20 November 2004
Available online 26 January 2005

Abstract

Platinum supported on high surface area tungsten trioxide (WO_3) has received intensive attention in recent years, mainly because of its improved tolerance towards carbon monoxide (CO) poisoning during methanol oxidation and its enhanced electrocatalytic activity. However, the chemical instability of WO_3 in acid medium is a major issue that hinders its application in fuel cell electrodes. In the present work, the stability of WO_3 is shown to be improved by suitable Ti^4 substition in the WO_3 framework. However, the improvement in the stability of WO_3 in acid medium was found to be significant only at lower amounts of Ti^4 in the framework. On the other hand, the electrocatalytic activity of Pt loaded $W_{1-x}Ti_xO_3$/C ($x = 0.0$, 0.05, 0.09 and 0.17) for methanol oxidation, evaluated by cyclic voltammetry, in acid medium follows the order: Pt–$W_{0.83}Ti_{017}O_3$/C > Pt–WO_3/C > Pt–$W_{0.91}Ti_{0.09}O_3$/C ∼ Pt–$W_{0.95}Ti_{0.05}O_3$/C. The trend in the activity observed correlates well with that of the increase in the ohmic resistance of the electrode determined by electrochemical impedance spectroscopy.

Keywords: Fuel cell; Methanol oxidation; Tungsten trioxide dissolution; Pt–WO_3/C; Electrocatalyst; DMFC

1. Introduction

Platinum supported on high surface area tungsten trioxide (WO_3) has received intensive attention in recent years, mainly because of its potential utility in anodes in direct methanol fuel cells [1–4]. The electrocatalytic activity for methanol oxidation was enhanced when platinum is supported on WO_3 [5,6]. The reason for choosing transition metal oxides such as WO_3 as a support for platinum is because of the fact that these oxides can form tungsten bronzes, thereby making the dehydrogenation of methanol more effective and also the oxophilic nature of the oxide helps in removing the adsorbed intermediates during the methanol oxidation [7]. Although, these systems show better tolerance towards poisoning by the adsorbed intermediates, the dissolution of WO_3 in the acidic medium under the operating conditions is responsible for poor stability [8]. The dissolution of amorphous WO_3 in acid medium takes place even under open circuit conditions. However, the dissolution of the WO_3 is undesirable for use as anode material. The stability of WO_3 in acid medium can be improved by (i) coating the electrode with a thin layer of Nafion [9], (ii) by suitable substitution of transition metal ions in the frame work of WO_3 [10–13] and (iii) by intercalating composite material based on inorganic compound and conducting polymers [14].

Generally, the anodic dissolution of oxide (semiconductor) electrodes requires the capture of valence band holes in surface bonds [15,16]. Anodic dissolution depends on the rate of hole capture by the oxide electrode at the interface, which in turn depends on the extent of band bending at the electrode/electrolyte interface on the anodic bias. If the band bending is small on the oxide surface, the probability of electron or hole tunnelling will be very small hence, leading to little dissolution in the aqueous medium.

The dissolution studies of the oxides substituted with various transition metal ions such as Fe, Co, Ni, Mn and Ti in acid, and alkaline media are reported in the literature [17]. The substitution of Ni, Co and Ti on the oxide framework

* Corresponding author. Tel.: +91 44 22578250; fax: +91 44 22578250.
E-mail addresses: bvnathan@iitm.ac.in, bviswanathan@hotmail.com (B. Viswanathan).

0378-7753/$ – see front matter © 2004 Elsevier B.V. All rights reserved.
doi:10.1016/j.jpowsour.2004.11.033

suppresses the dissolution by decreasing the probability of electron/hole tunnelling at the interface. Thus, the dissolution reaction at the high anodic potentials can be suppressed by suitable transition metal ion substitution. Since, Ti^{4+} is stable in acid medium, it was considered worthwhile to study the stability of WO_3 substituted with Ti^{4+} in the oxide framework. Moreover, it is shown in the literature [18] that the life time of the WO_3 electrode was improved five times when Ti^{4+} incorporated in the oxide framework. Also, the Ti substituted $SrFe_{0.9}M_{0.1}O_3$ system is shown to exhibit little dissolution compared to that of the unsubstituted $SrFeO_3$ in aqueous solutions [17].

In the present investigation, various amounts of titanium incorporated WO_3 crystallized in the monoclinic phase has been used as a support for the platinum and investigated for the electrooxidation of methanol in acid. The material was characterized by X-ray diffraction (XRD), UV–vis spectroscopy, X-ray photoelectron spectroscopy (XPS), cyclic voltammetry and electrochemical impedance spectroscopy. The evaluation of the electrocatalytic activity for methanol oxidation and electrochemical stability of WO_3, with and without Ti^{4+} incorporation, was carried out using cyclic voltammetry. Chronoamperometric measurements were also carried out to evaluate the stability of Pt supported Ti-incorporated WO_3 during methanol oxidation in acidic medium, by fixing the oxidation potential.

2. Experimental

2.1. Synthesis of Pt–$W_{1-x}Ti_xO_3$/carbon (x = 0.06, 0.09 and 0.17, and Pt:W = 1:1)

The preparation of the composite material involves two steps (i) preparation of Ti incorporated WO_3 on carbon support and (ii) loading of Pt on Ti-incorporated WO_3 supported on carbon.

2.1.1. Synthesis of Ti incorporated WO_3

Peroxopolytungstic acid was obtained by the dissolution of commercial tungstic acid H_2WO_4 (S.d. fine chemicals) powder in an aqueous solution of hydrogen peroxide (30%). Dissolution was performed for a few hours at 50 °C until a clear colorless acid solution was obtained. The dissolution of tungstic acid in hydrogen peroxide leads to the formation of peroxo-polytungstic acid species, which is stable as long as hydrogen peroxide is in excess. The titanium incorporated WO_3 ($W_{1-x}Ti_xO_3$, where $x = 0.06$, 0.09 and 0.17) phases were formed on the carbon support by adding stoichiometric amount of titanium isopropoxide (Fluka) to the peroxo-polytungstic acid solution in appropriate Ti:W ratio, to which carbon (Vulcan XC 72 R) was added. Mixing of titanium and tungsten sources were carried out in ice-cooled beaker, as the reaction is exothermic. No precipitation was found to occur. The peroxo species was then decomposed at 60 °C to allow the titanium incorporated WO_3 to get precipitated on the carbon support. The sample was then calcined at 450 °C for 2 h in air.

2.1.2. Loading of Pt on the $W_{1-x}Ti_xO_3$/carbon (x = 0.0, 0.05, 0.09 and 0.17)

To 500 mg of Ti-incorporated WO_3/C, the required amount of aqueous hexachloroplatinic acid (H_2PtCl_6), obtained from Arora Mathey, to keep the Pt:W ratio 1:1 was added, followed by evaporation to dryness at 60 °C. The resulting material was then reduced in hydrogen atmosphere at 350 °C for 4 h.

2.2. Spectroscopic characterization of the Ti-incorporated WO_3 supported carbon

The XRD analyses of the all the samples prepared were carried out on a Rigaku miniflex instrument using Fe-filtered Co kα (λ = 1.7902 Å) radiation (35 kV, 25 mA) at room temperature for the powdered samples.

UV–vis spectra for the samples were recorded using a Perkin-Elmer spectrophotometer in the range of 200–400 nm for the powder samples ($W_{1-x}Ti_xO_3$/C) in nujol mode. A small quantity of the sample was initially mixed with nujol and the semi-solid paste was then spread on to the Whatmann filter paper and kept in the sample cell. The Whatmann filter paper, to which the nujol was spread, is kept in the reference cell. Then the spectra were recorded.

The X-ray photo electron spectroscopic studies were performed using an Axis Ultr Kratos Instrument using Al kα as X-ray source. The etching experiments were performed at 2 kV and 15 mA and sputtered with Ar at a pressure of 5×10^{-8} mbar.

2.3. Electrochemical studies

The electrochemical oxidation of methanol was carried out using cyclic voltammetry (Potentioscan Wenking Model POS 73) in 1 M H_2SO_4 and 1 M CH_3OH mixture at RT. The reference and counter electrodes used in the present work were saturated Ag/AgCl and Pt (1.5 cm^2 area), respectively.

The electrode was prepared as follows; 20 mg of oxide was dispersed in 0.5 ml-distilled water and ultrasonicated for 30 min. From the dispersion, 20 μl dispersion was taken on the glassy carbon surface (Ø 1 mm diameter) and dried in air followed by the addition of 5 μl of 5% Nafion solution as binder. Chronoamperometric responses were obtained by fixing the potential and recording the current response with time using Philips X-t recorder.

The electrochemical impedance measurements were carried out using Autolab PGSTAT30 with an FRA software program between 5 mHz and 100 kHz with an ac arc of 5 mV peak to peak overlap on a dc bias potential and the impedance data were recorded with the change in the frequency. The ohmic resistance (Ω cm^2) and charge transfer

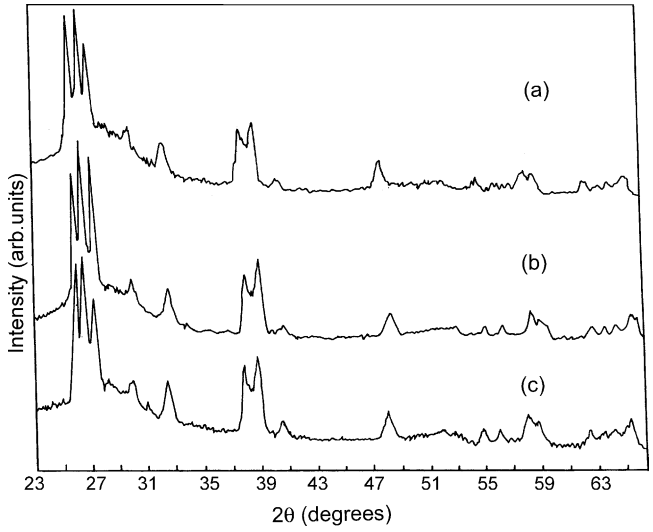

Fig. 1. X-ray diffraction pattern observed for the compositions: (a) $W_{0.95}Ti_{0.05}O_3$/C, (b) $W_{0.91}Ti_{0.09}O_3$/C and (c) $W_{0.83}Ti_{0.17}O_3$/C.

resistance ($\Omega\,cm^2$) and the capacitance were obtained from the real part of the impedance (*x*-axis) in the Nyquist plot.

3. Results and discussion

3.1. X-ray diffraction studies

The X-ray diffraction pattern obtained for the Ti-incorporated WO_3 with varying titanium contents, before loading Pt, is shown in Fig. 1. All the Ti-incorporated WO_3 compositions crystallize in stable monoclinic form on the carbon support. The pattern obtained is well in agreement with the literature reports (JCPDS file no. 24-747). No impurity phases were found to exist on the carbon support.

3.2. UV–vis spectroscopy

The UV–vis spectra were measured for the samples $W_{1-x}Ti_xO_3$/C (where $x = 0.0$, 0.05, 0.09 and 0.17) in nujol mode, in order to check the presence of titanium ions in the WO_3 framework. The UV–vis spectra of the Ti-incorporated WO_3 samples measured are shown in Fig. 2a–c. For comparison, the UV–vis spectra of the samples of WO_3 without Ti and bulk titanium dioxide, prepared on the carbon support by the same procedure, are also included, respectively, in Fig. 2d and e. The absence of signal at around 220–230 nm for the Ti-incorporated WO_3 supported on carbon samples (Fig. 2a–c) suggests the titanium is present in the WO_3 framework. This is also evident from the Fig. 2d and e that a signal with a maximum at about 223 nm is characteristic of bulk titanium dioxide (Fig. 2e), while no signal is seen on the WO_3 without titanium (Fig. 2d) [19].

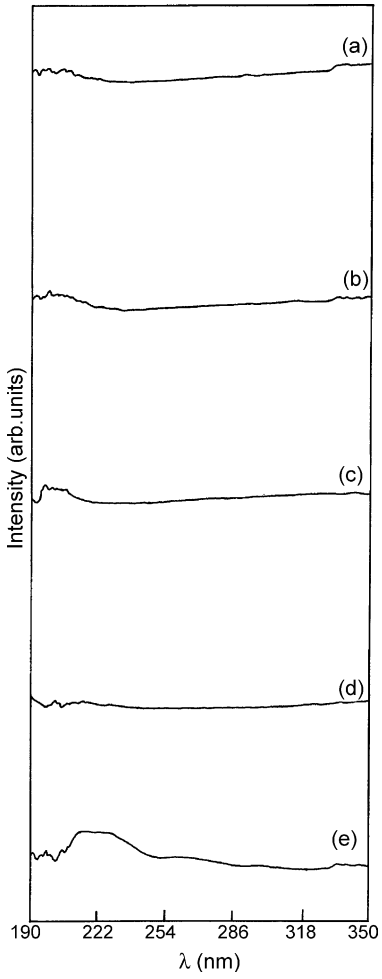

Fig. 2. UV–vis spectra taken in nujol for the electrodes of compositions: (a) $W_{0.95}Ti_{0.05}O_3$/C, (b) $W_{0.91}Ti_{0.09}O_3$/C, (c) $W_{0.83}Ti_{0.17}O_3$/C, (d) WO_3/C and (e) TiO_2/C.

3.3. X-ray photoelectron spectroscopic characterization of Pt–$W_{1-x}Ti_xO_3$/carbon

In order to find out the oxidation states of Pt, W and Ti, the X-ray photoelectron spectra were recorded for the Pt loaded on WO_3 compositions supported on carbon with and without Ti incorporation, taken in Pt 4f, W 4f and Ti 2p region, and were shown in Fig. 3 (Pt–WO_3/C), Fig. 4 (Pt–$W_{0.95}Ti_{0.05}O_3$/C), Fig. 5 (Pt–$W_{0.91}Ti_{0.09}O_3$/C) and Fig. 6 (Pt–$W_{0.83}Ti_{0.17}O_3$/C). The XP spectra recorded in the Pt 4f region (Fig. 3a) of the sample Pt–WO_3/C show two peaks with binding energies centered at 71.8 eV ($4f_{7/2}$) and 75.1 eV ($4f_{5/2}$), suggesting that the platinum particles are present in the metallic state. The XPS spectra recorded in the W 4f region (Fig. 3b) of the sample Pt–WO_3/C show two peaks with binding energies centered at 35.5 ($4f_{7/2}$) and 37.5 eV ($4f_{5/2}$), suggesting the presence of tungsten in the +VI oxidation state.

The XP spectra recorded in the Pt 4f region (Fig. 4a and Fig. 5a) of the samples Pt–$W_{0.95}Ti_{0.05}O_3$/C and Pt–$W_{0.91}Ti_{0.09}O_3$/C, show two peaks with binding energies

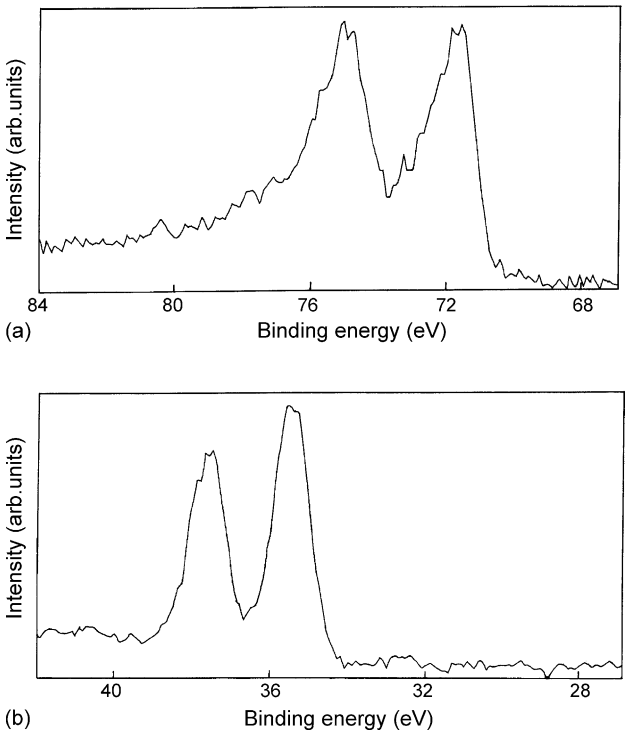

Fig. 3. X-ray photoelectron spectra of Pt–WO_3/C taken in (a) Pt 4f region and (b) W 4f region.

centered at 71.4 ($4f_{7/2}$) and 74.8 eV ($4f_{5/2}$), which are characteristic of the metallic platinum. The two characteristic peaks observed in the W 4f region (Figs. 4b and 5b) with binding energies centered at 35.7 ($4f_{7/2}$) and 37.9 eV ($4f_{5/2}$), suggest the presence of tungsten in the +VI oxidation state. The XP spectra in Ti 2p region (Fig. 4c and 5c) shows no characteristic signals, suggesting that the Ti may not be present on the surface, instead it may be present in the bulk of the WO_3 matrix or the Ti is covered with metallic Pt.

The XPS spectra recorded in the W 4f region (Fig. 6b) of the sample Pt–$W_{0.83}Ti_{0.17}O_3$/C show two peaks with binding energies centered at 35.5 ($4f_{7/2}$) and 37.5 eV ($4f_{5/2}$), suggesting the presence of tungsten in the +IV oxidation state. The XP spectra taken in the Ti 2p region (Fig. 6c) show two peaks with binding energies centered at 452.8 ($2p_{3/2}$) and 459.2 eV ($2p_{1/2}$), which reveals the presence of Ti in the metallic state. The presence of Ti in the metallic state may be due to the reduction of titanium ions present in the WO_3 lattice during the hydrogen reduction treatment at 350 °C, which was carried out for the reduction of platinum ions to metallic platinum. Thus, for the higher Ti containing WO_3 compositions, the Ti that was present inside the oxide framework (UV–vis) may no longer be stable and will come out of the framework as metallic Ti during the hydrogen reduction treatment. The XP spectra taken in the Pt 4f region (Fig. 6a) show no characteristic signals, probably suggesting the absence of platinum on the surface or the platinum is covered with metallic Ti.

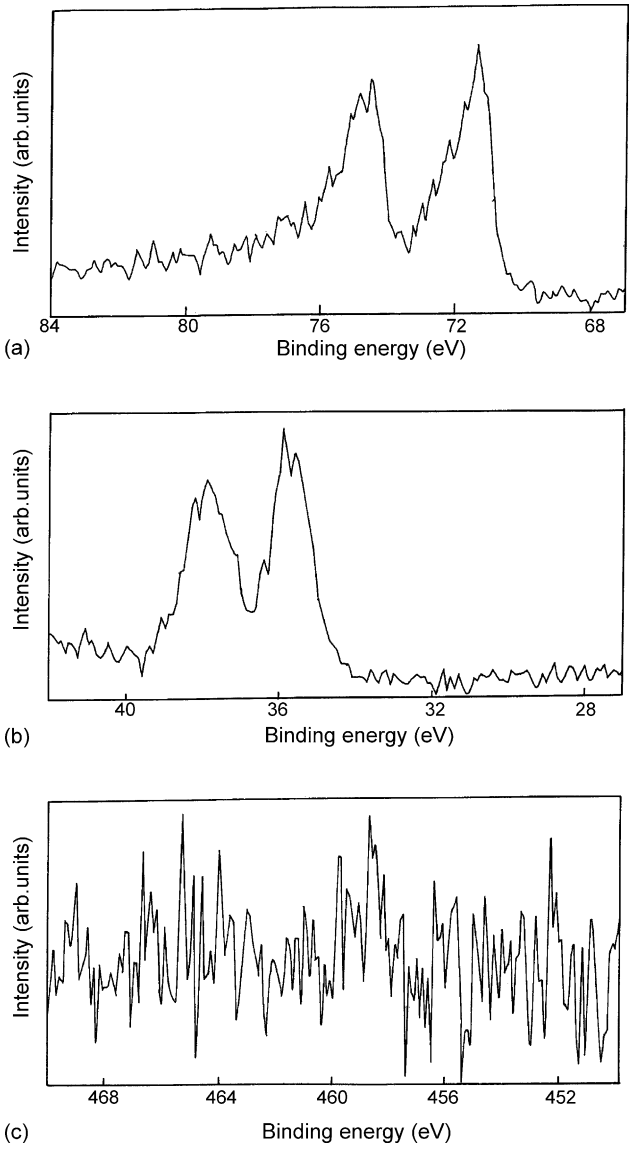

Fig. 4. X-ray photoelectron spectra of Pt–$W_{0.95}Ti_{0.05}O_3$/C taken in (a) Pt 4f region, (b) W 4f region and (c) Ti 2p region.

3.4. Estimation of platinum on the composite electrode

The platinum loading on the composite electrode were determined using $SnCl_2$ method [20]. A known amount of Pt–$W_{1-x}Ti_xO_3$ (where $x = 0.05$, 0.09 and 0.17) supported on carbon was treated at 800 °C for 5 h in air to burn the carbon. The Pt metal was extracted using aqua regia. The concentrated HCl was added followed by evaporating to dryness; this was repeated for three to four times to ensure complete extraction of Pt. This was then made up to known volume. From that 5 ml of aliquot was taken and 5 ml of 10% $SnCl_2$ solution was added and the absorbance was measured at 403 nm. The amount of Pt was determined by constructing calibration plot with known amounts of H_2PtCl_6. The amount of platinum present in the 50 mg of the catalysts is shown in Table 1.

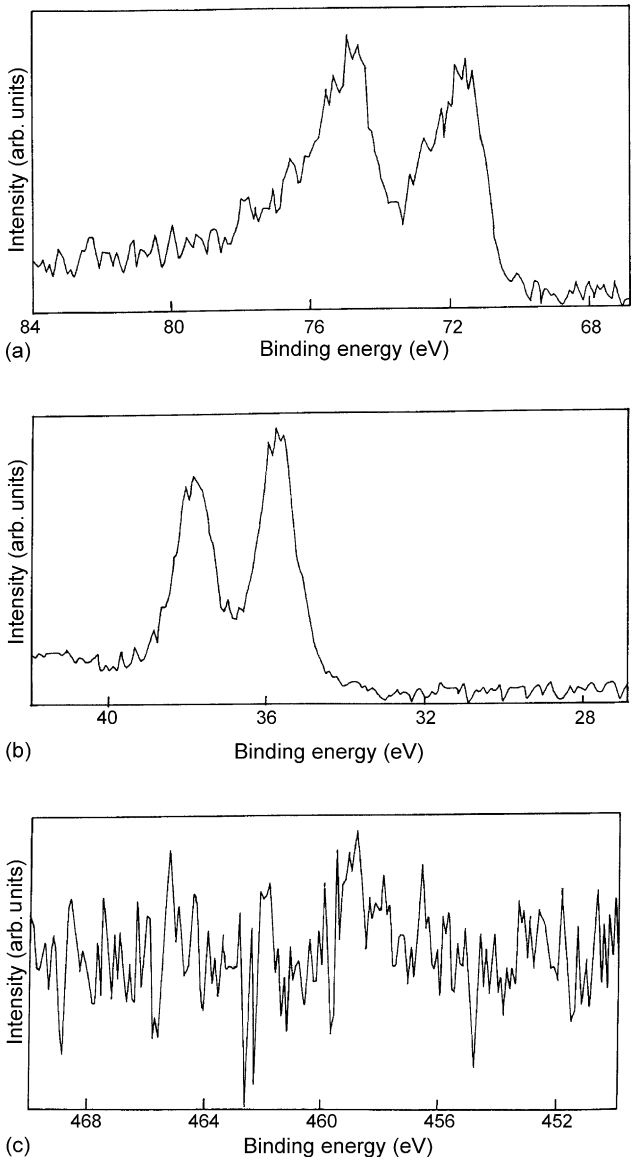

Fig. 5. X-ray photoelectron spectra of Pt–$W_{0.91}Ti_{0.09}O_3$/C taken in (a) Pt 4f region, (b) W 4f region and (c) Ti 2p region.

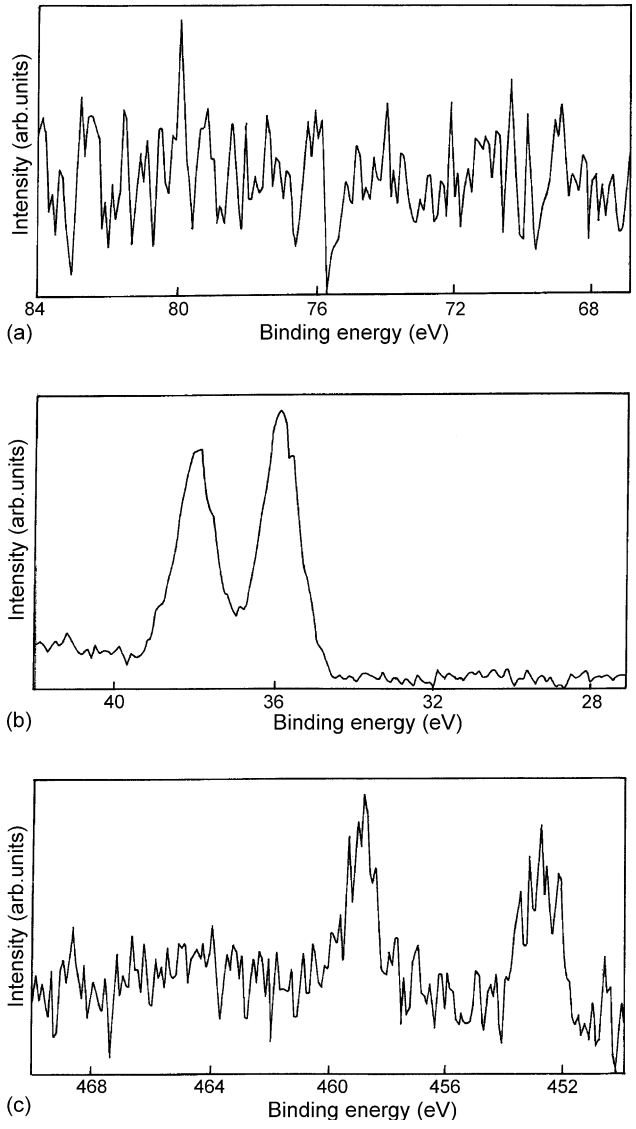

Fig. 6. X-ray photoelectron spectra of Pt–$W_{0.83}Ti_{0.17}O_3$/C taken in (a) Pt 4f region, (b) W 4f region and (c) Ti 2p region.

3.5. Electrochemical characterization of Ti incorporated WO_3 supported carbon

The cyclic voltammogram of $W_{1-x}Ti_xO_3$/C ($x = 0.0$, 0.05, 0.09 and 0.17) recorded in 1 M sulfuric acid, at a scan rate of 25 mV s^{-1} is shown in Fig. 7a–d. The electrochemical response of tungsten observed at −0.15 V during the forward scan for the electrode WO_3/C (Fig. 7a) is in agreement with the literature reports [21,22]. In the case of Ti-incorporated WO_3 (Fig. 7b–d), the electrochemical response due to the tungsten is observed at higher potential (0.0 V). This may be due to the incorporation of titanium in the WO_3 frame work, which alters the peak potential of the tungsten redox reaction.

3.6. Electrochemical methanol oxidation

Fig. 8a–d shows the cyclic voltammogram of platinum loaded $W_{1-x}Ti_xO_3$/C (where $x = 0.0$, 0.05, 0.09 and 0.17) in 1 M H_2SO_4, before the addition of methanol, recorded at a scan rate of 25 mV s^{-1} in the potential range −0.4 to +0.8 V versus Ag/AgCl. A broad peak at around −0.1 V is due to the

Table 1
Amount of platinum in 50 mg of the Pt–$W_{1-x}Ti_xO_3$/C ($x = 0$, 0.05, 0.09 and 0.17) catalyst

Catalyst	Platinum loading (mg)
Pt–WO_3/C	3.85
Pt–$W_{0.95}Ti_{0.05}O_3$/C	3.77
Pt–$W_{0.91}Ti_{0.09}O_3$/C	2.80
Pt–$W_{0.83}Ti_{0.17}O_3$/C	1.32

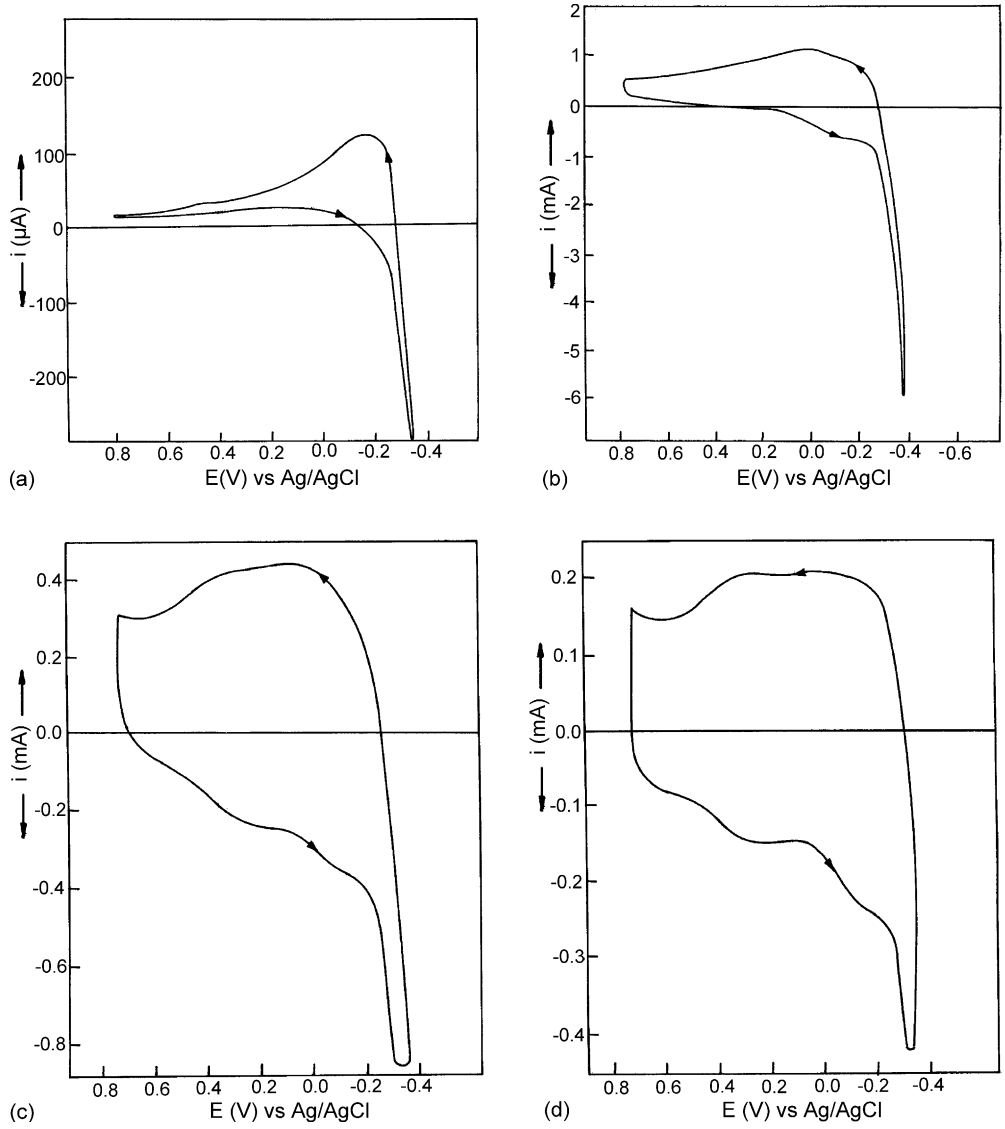

Fig. 7. Cyclic voltammogram recorded in 1 M H_2SO_4 for the compositions: (a) WO_3/C, (b) $W_{0.95}Ti_{0.05}O_3$/C, (c) $W_{0.91}Ti_{0.09}O_3$/C and (d) $W_{0.83}Ti_{0.17}O_3$/C at RT at a scan rate of 25 mV s^{-1}.

hydrogen desorption from the platinum surface as well as the redox transition of W^{5+}/W^{6+}. In the presence of methanol (Fig. 9a–d), the methanol oxidation starts at +0.2 V for all the platinum loaded $W_{1-x}Ti_xO_3$ (where $x = 0.0$, 0.05, 0.09 and 0.17) samples and the current increases with increase in the applied potential during the forward scan. All the catalysts exhibit the irreversible nature of the methanol electrooxidation. The mass activity (mA mg^{-1}) of the platinum catalyst for methanol oxidation is defined as the current (mA) obtained from the forward cyclic voltammogram scans per unit mass (mg) of platinum. The specific and mass activities of the composite electrodes were compared in Table 2. For comparison, the cyclic voltammogram obtained for the methanol oxidation on 5% Pt/C is also shown in Fig. 10. The cyclic voltammograms reported here are reproducible. It is seen from the Table 2 that the Pt–WO_3/C shows higher activity compared to that of the Pt/C as reported in the literature [1–4]. The improvement in the activity exhibited by Pt–WO_3 is due to the enhancement in the dehydrogenation of methanol as tungsten trioxide is capable of forming tungsten bronzes (H_xWO_{3-x}). For the Ti-incorporated WO_3 supports for platinum, the activity was found to increase with increase in the Ti content in the oxide. Initially there is decline in the activity at lower titanium contents ($x = 0.05$ and 0.09) and later the activity was found to be increased for the higher Ti containing composition, Pt–$W_{0.83}Ti_{017}O_3$/C ($x = 0.17$), when compared to that of the Pt–WO_3/C. The activity for methanol oxidation follows the order: Pt–$W_{0.83}Ti_{017}O_3$/C > Pt–WO_3/C > Pt–$W_{0.91}Ti_{0.09}O_3$/C ∼ Pt –$W_{0.95}Ti_{0.05}O_3$/C. In order to account for the higher activity exhibited by the Pt–$W_{0.83}Ti_{017}O_3$/C, the electrochemical impedance spectroscopic measurements were carried out to determine the ohmic resistance of the electrode and the charge transfer resistance for the methanol oxidation.

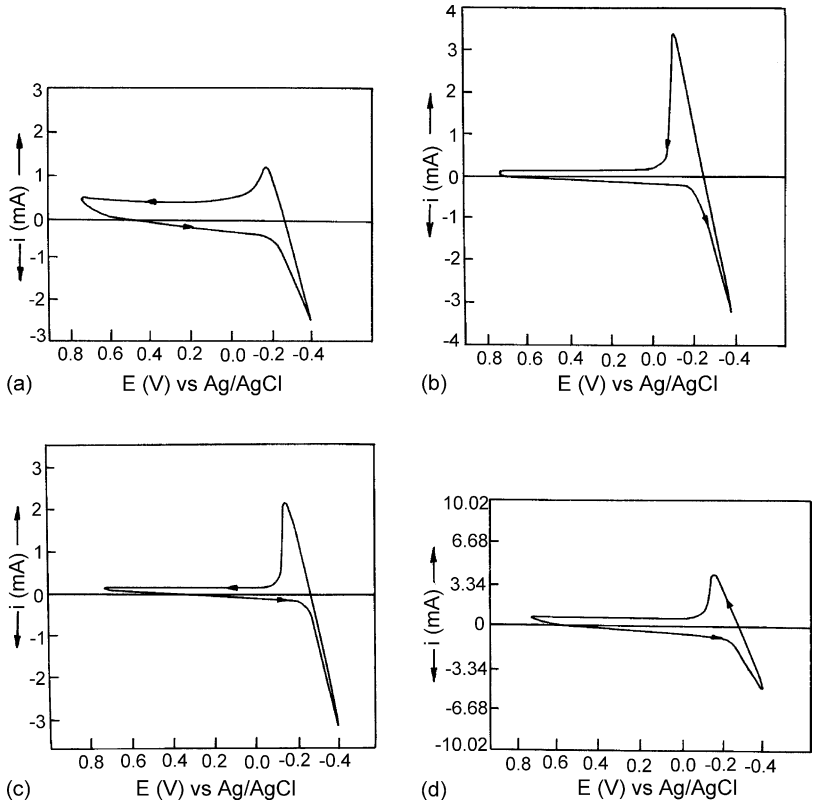

Fig. 8. Cyclic voltammogram obtained for various amounts of Ti-incorporated WO_3 as supports for platinum in 1 M H_2SO_4 (a) Pt–WO_3/C, (b) Pt–$W_{0.95}Ti_{0.05}O_3$/C, (c) Pt–$W_{0.91}Ti_{0.09}O_3$/C and (d) Pt–$W_{0.83}Ti_{0.17}O_3$/C at RT at a scan rate of 25 mV s^{-1}.

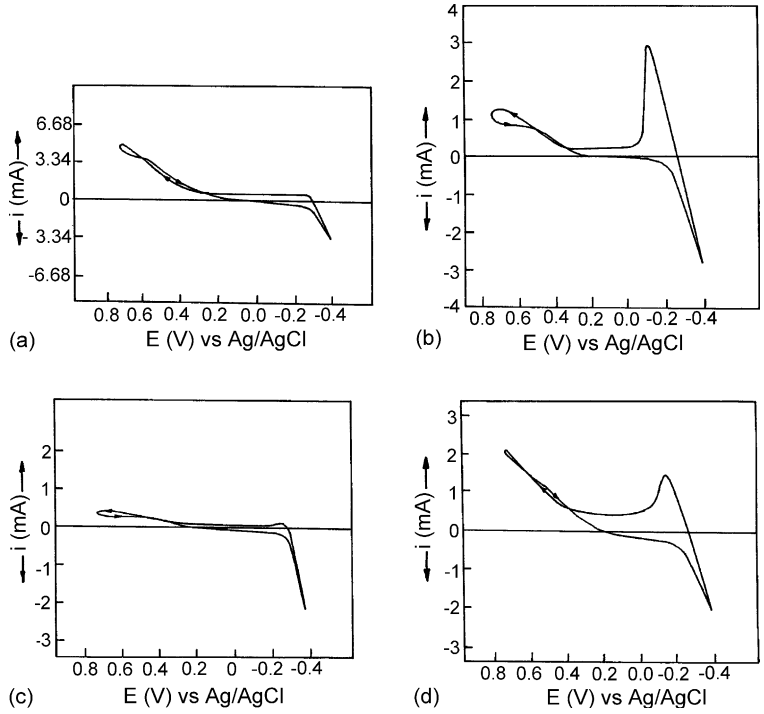

Fig. 9. Cyclic voltammogram obtained for various amounts of Ti-incorporated WO_3 as supports for platinum in 1 M H_2SO_4 and 1 M CH_3OH mixture (a) Pt–WO_3/C, (b) Pt–$W_{0.95}Ti_{0.05}O_3$/C, (c) Pt–$W_{0.91}Ti_{0.09}O_3$/C and (d) Pt–$W_{0.83}Ti_{0.17}O_3$/C, at RT at a scan rate of 25 mV s^{-1}.

Table 2
Methanol oxidation activity comparison of Pt–$W_{1-x}Ti_xO_3$ (where $x = 0.0$, 0.05, 0.09 and 0.17) supported carbon

Electrocatayst	Amount of Pt (μg)	Specific activity (I_s) (mA cm^{-2}) at +0.6 V vs. Ag/AgCl	Mass activity (I_m) (mA mg^{-1} Pt) at +0.6 V vs. Ag/AgCl
Pt/C	40	43	75.3
Pt–WO_3/C	60	106	123.7
Pt–$W_{0.95}Ti_{0.05}O_3$/C	60	33	38.5
Pt–$W_{0.91}Ti_{0.09}O_3$/C	45	24	70.0
Pt–$W_{0.83}Ti_{017}O_3$/C	21	41	136.7

3.7. Electrochemical impedance

The electrochemical impedance spectroscopic measurements were carried out in 1 M H_2SO_4 and 1 M CH_3OH mixture for the samples Pt–$W_{1-x}Ti_xO_3$/C (where $x = 0.0$, 0.05, 0.09 and 0.17), by fixing the methanol electrooxidation potential at +0.4 V, in the frequency range of 5 mHz–100 kHz. The ohmic resistance of the Pt–$W_{1-x}Ti_xO_3$/C (where $x = 0.0$, 0.05, 0.09 and 0.17) was obtained from the real part of the impedance obtained at high frequency and were tabulated in Table 3. The data reveal that the ohmic resistance decreases with increase in the Ti^{4+} substitution in the WO_3 framework. The value of ohmic resistance is higher for the electrode of compositions (Pt–$W_{0.95}Ti_{0.05}O_3$/C and Pt–$W_{0.91}Ti_{0.09}O_3$/C), which has lower Ti^{4+} amounts in the framework and almost comparable value for the composition (Pt–$W_{0.83}Ti_{017}O_3$/C) that possess higher Ti content when compared with that of the Pt–WO_3 electrode. The decrease in the ohmic resistance at the higher Ti^{4+} containing composition (Pt–$W_{0.83}Ti_{017}O_3$/C), which is comparable to that of the Pt–WO_3/C, could be to be due to the presence of metallic titanium on the surface as is evident from the X-ray photoelectron spectroscopic study (Fig. 6c).

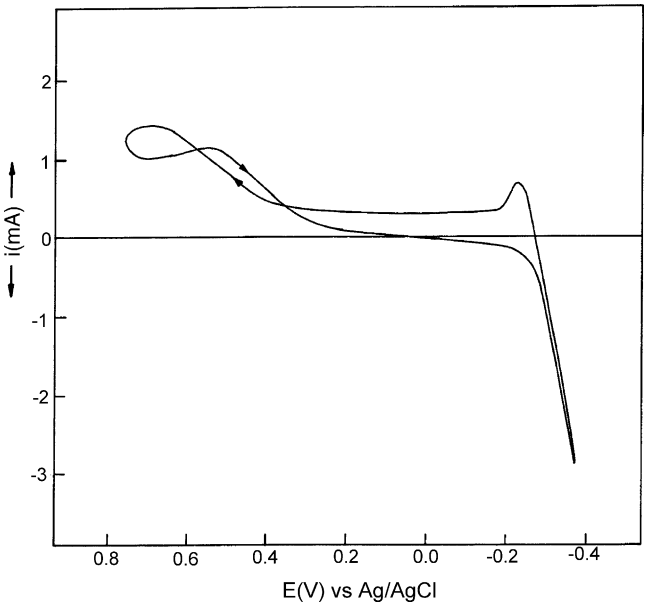

Fig. 10. Cyclic voltammogram obtained for 5% Pt/C 1 M H_2SO_4 and 1 M CH_3OH mixture at RT at a scan rate of 25 mV s^{-1}.

The charge transfer resistance obtained from the Nyquist plot, for the Pt–$W_{1-x}Ti_xO_3$/C (where $x = 0.0$, 0.05, 0.09 and 0.17) at the methanol oxidation potential, were also tabulated in Table 3. The R_{ct} was found to be higher for the Ti incorporated WO_3 supports at lower titanium contents ($x = 0.05$ and 0.09) compared to that of the unsubstituted WO_3 and for x is 0.17. The decrease in the charge transfer resistance for the composite electrodes was found to have good correlation with the increase in the electrocatalytic activity for methanol oxidation in acid medium.

3.8. Chronoamperometric response

The chronoamperometric measurements were carried out during the methanol oxidation with the composite electrodes, at a fixed methanol electrooxidation potential of +0.4 V versus Ag/AgCl and are shown in Fig. 11a (Pt–WO_3/C), Fig. 11b (Pt–$W_{0.95}Ti_{0.05}O_3$/C) and Fig. 11c (Pt–$W_{0.91}Ti_{0.09}O_3$/C). The chronoamperometric response for the composition Pt–$W_{0.95}Ti_{0.05}O_3$/C is not shown. It is seen from the Fig. 11(a–c) that the current initially decays with time and then becomes stable. The decay in the current is due to the accumulation of oxidation byproducts or residues that poisons the Pt sites [22]. Although several poisons have been identified from mechanistic studies, carbon monoxide (CO) is often cited as the leading cause of catalyst poisoning as it binds irreversibly to the platinum catalyst and thereby, reduces the number of sites available for methanol electrooxidation. The oxophilic nature of the WO_3 helps in removing the adsorbed intermediates during the methanol oxidation. Since WO_3 undergoes dissolution in the acid medium, the decrease in the activity can attributed to the poor tolerance of the composite electrode towards CO poisoning because of the dissolution of the tungsten in the solution. From the slope of the current decaying region, the rate of deactivation of the composite electrodes were calculated and is shown in

Table 3
Impedance parameters obtained for the Pt–$W_{1-x}Ti_xO_3$/C (where $x = 0.0$, 0.05, 0.09 and 0.17) for methanol oxidation in acid media

Electrocatalyst	Ohmic resistance (Ω cm^2)	Charge transfer resistance (R_{ct}) (Ω cm^2)
Pt–WO_3/C	0.39	0.77
Pt–$W_{0.95}Ti_{0.05}O_3$/C	0.57	1.05
Pt–$W_{0.91}Ti_{0.09}O_3$/C	0.63	0.81
Pt–$W_{0.83}Ti_{017}O_3$/C	0.39	0.21

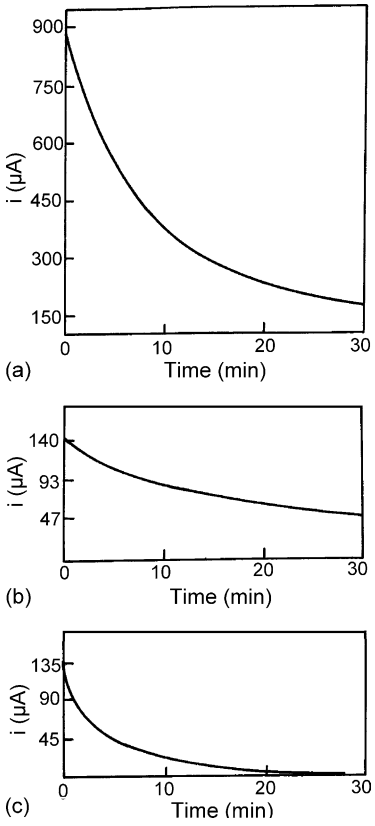

Fig. 11. Chronoamperometric response during methanol oxidation on the electrode of composition (a) Pt–WO_3/C, (b) Pt–$W_{0.95}Ti_{0.05}O_3$/C, (c) Pt–$W_{0.91}Ti_{0.09}O_3$/C, polarized at +0.4 V vs. Ag/AgCl.

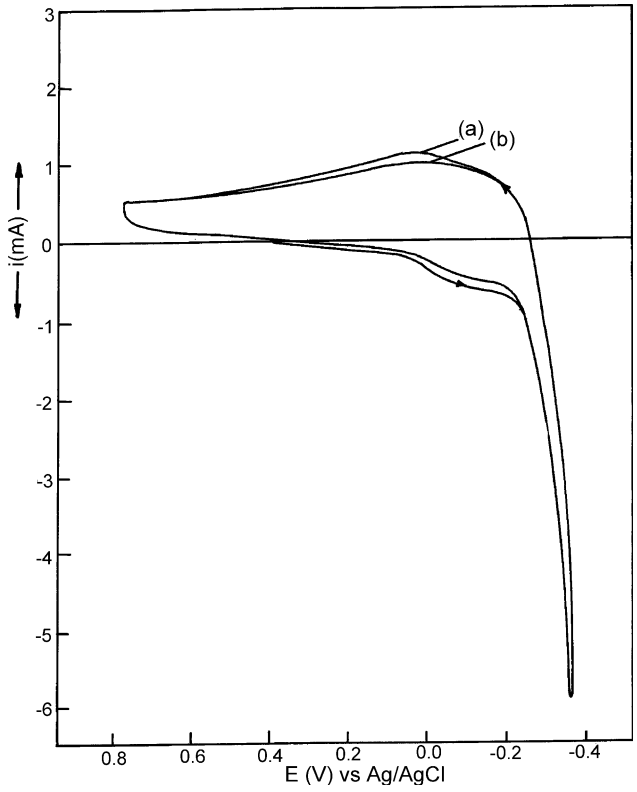

Fig. 12. Cyclic voltammogram recorded for the electrode of composition $W_{0.95}Ti_{0.05}O_3$/C in 1 M H_2SO_4 at RT (a) before and (b) after cycling for 2 h in the potential range of −0.4 to +0.8 V vs. Ag/AgCl, at a scan rate of 25 mV s^{-1}.

Table 4. The lesser value of the rate of deactivation of the Pt supported on the Ti-incorporated WO_3 composite electrodes (Table 4) compared to that of the Pt–WO_3 electrode, during methanol oxidation, indicate better electrode stability of WO_3 in the presence of Ti in acid medium. The improvement in the stability could be due to the decrease in the dissolution of tungsten in the presence of Ti^{4+} in the tungsten trioxide. However, the rate of deactivation is found to be less only when the titanium is present at lower amounts in the WO_3 framework (Table 4). This could probably be due to the instability of Ti^{4+} in the oxide framework, especially at higher amounts (0.17), that undergoes reduction and gets accumulated as metallic Ti during the hydrogen treatment, which was carried out for the reduction of platinum ions to Pt.

Fig. 12 shows the cyclic voltammogram recorded for the typical electrode $W_{0.95}Ti_{0.05}O_3$/C, before and after polarizing at +0.4 V versus Ag/AgCl for 2 h in the acid medium. The nature of cyclic voltammogram and the magnitude of the current response almost remain same before (Fig. 12a) and after (Fig. 12b) polarizing the electrode, suggesting that there is no appreciable leaching in the acid medium under the present operating conditions.

Table 4
Rate of deactivation of Pt–$W_{1-x}Ti_xO_3$/C (where x = 0.0, 0.05, 0.09 and 0.17) for methanol oxidation in acid medium during anodic polarization

Electrocatalyst	Rate of deactivation (mA min^{-1}) polarized at +0.4 V vs. Ag/AgCl
Pt–WO_3/C	0.05
Pt–$W_{0.95}Ti_{0.05}O_3$/C	0.006
Pt–$W_{0.91}Ti_{0.09}O_3$/C	0.014
Pt–$W_{0.83}Ti_{017}O_3$/C	0.04

Cyclic voltammogram were also recorded after polarizing the electrode for 2 h at +0.4 V versus Ag/AgCl, for the compositions Pt–$W_{0.95}Ti_{0.05}O_3$/C (Fig. 13a), Pt–$W_{0.91}Ti_{0.09}O_3$/C (Fig. 13b) and Pt–$W_{0.83}Ti_{0.17}O_3$/C (Fig. 13c) in the presence of methanol. No significant variation in the activity for methanol oxidation is observed for the electrode of compositions Pt–$W_{0.95}Ti_{0.05}O_3$/C (Fig. 13a) and Pt–$W_{0.91}Ti_{0.09}O_3$/C (Fig. 13b), where the Ti^{4+} content is 0.05 and 0.09, respectively, when compared to that of the activity before the polarization (Fig. 9b and c). Whereas, a significant decline in the activity for methanol electrooxidation is noticed for the higher Ti^{4+} containing composition, Pt–$W_{0.83}Ti_{0.17}O_3$/C, (Fig. 13c) after polarization for 2 h, when compared to the activity that was obtained before polarization (Fig. 9d). The decline in the activity is due to the significant leaching of tungsten from the oxide matrix as the Ti^{4+} is not present in the oxide framework, instead it is present as metallic Ti on the surface. Hence the activity is no longer maintained for the higher Ti^{4+} containing composition, Pt–$W_{0.83}Ti_{0.17}O_3$/C, after polarizing it for 2 h at fixed potential. Thus, the stability

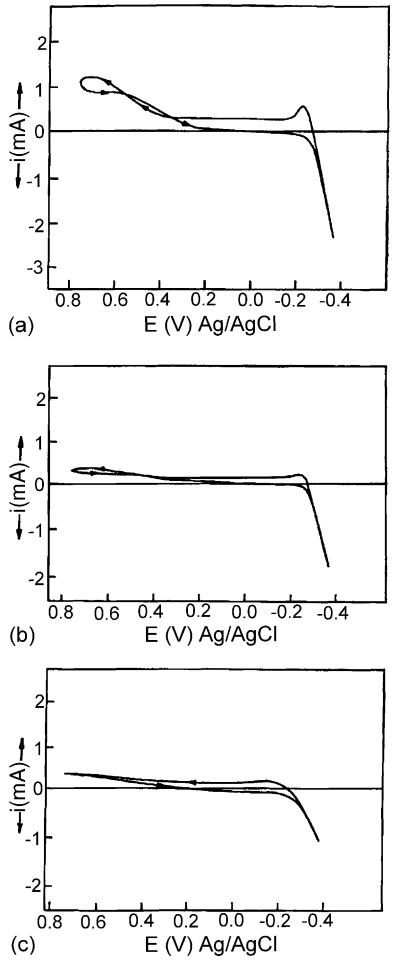

Fig. 13. Cyclic voltammogram recorded for the electrode of composition: (a) Pt–$W_{0.95}Ti_{0.05}O_3$/C, (b) Pt–$W_{0.91}Ti_{0.09}O_3$/C and (c) Pt–$W_{0.83}Ti_{0.17}O_3$/C, after the polarizing the electrode at +0.4 V vs. Ag/AgCl for 2 h, in 1 M H_2SO_4 and 1 M CH_3OH mixture, at RT at a scan rate of 25 mV s^{-1}.

of the tungsten trioxide is improved in the acid medium only when small an amount of Ti^{4+} is incorporated inside the oxide framework.

4. Conclusions

The stability of the WO_3 in the acid medium was found to be improved by transition metal ion substitution such as Ti^{4+} into the oxide framework. However, the improvement in the stability of the WO_3 is found to be better only when titanium is present in low amounts. At higher Ti^{4+} content, the Ti^{4+} is no longer stable in the oxide framework, which undergoes reduction during the hydrogen treatment. The improvement in the stability could be due to the alteration in the rate of hole capturing process of WO_3 by the Ti^{4+} at the interface, which is responsible for the dissolution of tungsten in acidic solution. The electrocatalytic activity for methanol oxidation, evaluated by cyclic voltammetry, was found to follow the order: Pt–$W_{0.83}Ti_{017}O_3$/C > Pt–WO_3/C > Pt–$W_{0.91}Ti_{0.09}O_3$/C $\sim$ Pt–$W_{0.95}Ti_{0.05}O_3$/C. The trend in the activity observed correlates well with that of the increase in the ohmic resistance of the electrode. The lower value of the ohmic resistance obtained for the electrode, Pt–$W_{0.83}Ti_{017}O_3$/C, is due to the accumulation of metallic titanium on the surface as evident from the XPS measurements.

References

[1] P.K. Shen, A.C. Tseung, J. Electrochem. Soc. 141 (1994) 3082–3090.
[2] P.K. Shen, P.K. Chen, A.C.C. Tseung, J. Chem. Soc., Faraday Trans. 90 (1994) 3089–3096.
[3] A. C. C. Tseung, P. K. Shen, J. Syed-Bokhari, US Patent 5470,673 (1995).
[4] A.K. Shukla, M.K. Ravikumar, A.S. Arico, G. Candiano, V. Antonucci, N. Giardano, A. Hammnett, J. Appl. Electrochem. 25 (1994) 528–532.
[5] P.J. Kulesza, L.R. Faulkner, J. Electroanal. Chem. 259 (1989) 81–98.
[6] P.J. Kulesza, L.R. Faulkner, J. Electrochem. Soc. 136 (1989) 707–713.
[7] A.C.C. Tseung, K.Y. Chen, Catal. Today 38 (1997) 439–443.
[8] B. Reichman, A.J. Bard, J. Electrochem. Soc. 126 (1979) 583–591.
[9] K.Y. Chen, A.C.C. Tsueng, J. Electrochem. Soc. 143 (1996) 2703–2707.
[10] K. Machida, M. Enyo, G. Adaci, J. Shiokawa, J. Electrochem. Soc. 135 (1981) 1955–1961.
[11] P.M.S. Monk, R.D. Partridge, R. Janes, M.J. Parker, J. Mater. Chem. 4 (1994) 1071–1074.
[12] P.K. Shen, J.S. Bokhari, A.C.C. Tseung, J. Electrochem. Soc. 138 (1991) 2778–2783.
[13] P.M.S. Monk, S.L. Chester, Electrochim. Acta 38 (1993) 1521–1526.
[14] M.G. Kanatzidis, C.G. Wu, J. Am. Chem. Soc. 111 (1989) 4139–4141.
[15] D. Vanmaekalbergh, P.C. Searson, J. Electrochem. Soc. 141 (1994) 697–702.
[16] H. Gerischer, Electrochim. Acta 35 (1990) 1677–1699.
[17] Y. Matsumoto, J. Kurimoto, E. Sato, Electrochim. Acta 25 (1979) 539–543.
[18] B. Yebka, B. Pecquenard, C. Julien, J. Livage, Solid State Ionics 104 (1997) 169–175.
[19] A. Chemseddine, R. Morineau, J. Livage, Solid State Ionics 9 (1983) 357–362.
[20] F.E. Beamish, J.C. Vanloon, Recent Advances in the Analytical Chemistry of the Noble Metals, Pergamon Press, Headington Hill, Hall, Oxford, 1972, p. 360–364 ;
A. Chemseddine, F. Babobnneau, J. Livage, J. Non Cryst. Solids 91 (1987) 271–278.
[21] M. Figlarz, Prog. Solid State Chem. 19 (1989) 1–46.
[22] S. Wasmus, J. Kuver, J. Electroanal. Chem. 461 (1999) 14–31.